

ACTIVATED CARBON ADSORPTION IN  
CIRCULAR AND TAPERED FIXED BEDS

by

KANG LING YONG

B.S., Kansas State University, 1987

---

A MASTER'S THESIS

submitted in partial fulfillment of the

requirements for the degree

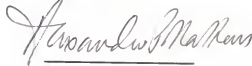
MASTER OF SCIENCE

Department of Civil Engineering

KANSAS STATE UNIVERSITY  
Manhattan, Kansas

1989

Approved by:



Major Professor



A11212 203615

## ABSTRACT

LD 3662  
.74  
CONF  
175  
Y66  
1.2

Equilibrium studies on a single-solute system (phenol) were carried out. All the experiments were conducted at 25°C and pH 7 using tapwater passing through a carbon column. The water was boiled to destroy any microorganisms in the water. The isotherm data were then fitted by the three parameter isotherm equation.

Batch studies were conducted on a single solute system for single adsorbent sizes. The results were predicted by a computer program and geometric mean diameter was used for the different particle sizes.

Fixed-bed studies were conducted for single adsorbent sizes as well as for a mixture of adsorbent sizes in a single solute system. A modified mathematical model was used so that the equilibrium could be represented by the three parameter isotherm. The model was devoted to compare the performance of a column fixed bed for constant pH and temperature with different particle sizes. Breakthrough curves were analyzed for geometric mean diameters. In the case of a mixture of sizes, the model was analyzed for stratified bed layers.

Sensitivity analyses were carried out for the mixed sizes and the results showed that if  $k_f$  (film transfer coefficient) is smaller than the calculated value, it becomes a controlling factor in the model. On the other hand, if  $k_f$  is greater than the calculated value, then  $D_s$  (solid phase diffusion coefficient) takes over as the rate limiting factor in the model.

In the tapered bed studies, the operating conditions were kept the same as the circular bed. The tapered bed showed significant

improvement in breakthrough time over the circular bed in both single and mixed sizes. The experimental data showed that for single sizes (#12/14), the tapered bed slowed the breakthrough time as much as 38% at  $C/C_0 = 0.1$ . Similarly, for the mixed sizes at  $C/C_0 = 0.1$ , the improvement was 18%. More detailed experimental and modeling studies need to be performed in the future to expand upon the results presented here.

## ACKNOWLEDGMENTS

The work reported herein has been supported by the Engineering Experiment Station of Kansas State University. This support is gratefully appreciated.

I would like to thank my adviser, Dr. A. P. Mathews for his hearty guidance and assistance in the graduate studies and completion of this thesis. I would also like to thank my committee members, Dr. A. J. Heber and Dr. J. K. Koelliker for their assistance.

Thanks are also extended to Mr. S.M. Lee who assisted in various stages of this research, I would also like to thank Mr. Jim Stone for his help during the experiments.

Finally, I would like to dedicate this research and thank my family for their affections, encouragements, and continuous moral support throughout my studies.

# Table of contents

	Page
LIST OF TABLES .....	III
LIST OF FIGURES .....	IV
CHAPTER 1 INTRODUCTION .....	1
1-1 General Discussion .....	1
1-2 Adsorption .....	2
1-3 Activation .....	2
1-4 Objectives of study .....	3
CHAPTER 2 REVIEW OF RELATED LITERATURE .....	4
2-1 Single solute adsorption models .....	4
2-1-1 Equilibrium models .....	4
2-1-2 Batch kinetic models .....	6
2-1-3 Kinetics for fixed beds .....	12
2-1-4 Fixed bed model .....	13
2-1-5 Solution of the model .....	14
2-1-6 Single solute fixed bed with two or more adsorbents .....	18
CHAPTER 3 EXPERIMENTAL MATERIALS AND METHODS .....	20
3-1 Materials .....	20
3-1-1 Adsorbent .....	20
3-1-2 Adsorbate .....	20
3-2 Methods .....	24
3-2-1 Analytical methods .....	24
3-2-2 Batch kinetic experiments .....	25
3-2-3 Equilibrium experiments .....	28

	3-2-4 Fixed bed experiments .....	30
	3-2-5 Tapered bed experiments .....	35
CHAPTER 4	RESULTS AND DISCUSSION .....	38
4-1	Equilibrium studies .....	38
4-2	Batch kinetic studies .....	38
4-3	Single solute studies for single sizes ...	43
	4-3-1 Column .....	43
	4-3-2 Tapered bed .....	44
4-4	Single solute studies for mixture of carbon sizes .....	44
	4-4-1 Column .....	44
	4-4-2 Sensitivity Analyses .....	53
	4-4-3 Tapered bed .....	53
CHAPTER 5	SUMMARY AND CONCLUSIONS .....	61
5-1	Summary and Conclusions .....	61
5-2	Recommendations .....	63
APPENDIX	.....	64
REFERENCES	.....	68
ABSTRACT	.....	

# LIST OF TABLES

	Page
3.1 Properties of the adsorbent .....	21
3.2 Carbon size fraction and diameter .....	22
3.3 Solute and its properties .....	23
3.4 Fixed bed operating conditions .....	32
4.1 Three parameter isotherm constants for phenol ..	39
4.2 External fixed-bed mass transfer coefficients and intraparticle diffusion coefficient for phenol adsorption for single adsorbent sizes ...	42
4.3 Fixed bed operating conditions for single size .....	45
4.4 Fixed bed operating conditions for mixed sizes .....	52

# LIST OF FIGURES

	Page
2.1 Adsorption on porous adsorbent --- rate limiting mechanisms .....	8
3.1 Schematic of batch kinetic system .....	26
3.2 Schematic of fixed bed adsorption system .....	31
3.3 Schematic of tapered bed adsorption system .....	36
3.4 Schematic of tapered bed .....	37
4.1 Adsorption isotherm for phenol at 25°C .....	40
4.2 Adsorption rate for phenol for carbon size #25/30 .....	41
4.3 Breakthrough curve for phenol adsorption in circular column for carbon size #12/14 .....	46
4.4 Breakthrough curve for phenol adsorption in circular column for carbon size #14/16 .....	47
4.5 Breakthrough curve for phenol adsorption in circular column for carbon size #16/18 .....	48
4.6 Breakthrough curve for phenol adsorption in circular column for carbon size #18/20 .....	49
4.7 Breakthrough curve for phenol adsorption for carbon size #12/14 for tapered bed and circular column .....	50
4.8 Breakthrough curve for phenol adsorption for carbon size #16/18 for tapered bed and circular column .....	51
4.9 Breakthrough curve for phenol adsorption for carbon mixed size #12/14, 14/16, #16/18 and #18/20 for circular column and tapered bed .....	54
4.10 Breakthrough curve for phenol adsorption in circular column for carbon mixed size #12/14, 14/16, #16/18 and #18/20. Prediction using average diameter and by layer .....	55



4.11	Breakthrough curve for phenol adsorption in circular column for carbon reverse mixed size #18/20, 16/18, #14/16 and #12/14. Prediction by layer .....	56
4.12	Breakthrough curve for phenol adsorption in circular column for carbon mixed size #12/14, 14/16, #16/18 and #18/20. Prediction by layer with $0.3k_f$ .....	57
4.13	Breakthrough curve for phenol adsorption in circular column for carbon reverse mixed size #18/20, 16/18, #14/16 and #12/14. Prediction by layer with $0.3k_f$ .....	58
4.14	Breakthrough curve for phenol adsorption in circular column for carbon mixed size #12/14, 14/16, #16/18 and #18/20. Prediction with $0.3k_f$ and $3k_f$ using average diameter .....	59
4.15	Breakthrough curve for phenol adsorption in circular column for carbon mixed size #12/14, 14/16, #16/18 and #18/20. Prediction with $0.5k_f$ and $2k_f$ using average diameter .....	60

## Chapter 1

### INTRODUCTION

#### 1-1 General Discussion

The discharge of chemicals and pesticides by industries into the environment will cause severe adverse effects including toxicity, carcinogenicity, taste and odor problems and degradation of the quality of water for consumptive use. In recent years, control of hazardous pollutants in water and wastewater treatment constitutes a matter of steadily expanding concern for the water quality specialist. Consequently, there is a need to develop more advanced technologies capable of removing these contaminants efficiently from water, to prevent further dispersion into the environment.

All organic contaminants cannot be regulated. Therefore, the Environmental Protection Agency (EPA) has developed a list of 129 chemical compounds (priority pollutants). The list is based on the following considerations:

- (a) quantity produced yearly,
- (b) physical and chemical properties,
- (c) frequency of occurrence in water,
- (d) availability of chemical standard and measurement,
- (e) toxicity, and
- (f) public interest.

A number of phenolic compounds occupy a prominent position on the EPA priority pollutant list. Apart from its toxicity, phenol is considered to contribute taste and odor problems in drinking water

with concentration as little as 2  $\mu\text{g/L}$ . Phenol can combine with the chlorite ion to produce chlorophenol.

Sources of phenolic compounds include effluents from coal-gas in steel plants, petroleum refineries, as well as a wide variety of industrial wastes from a process involving use of phenol as a raw material. On the other hand, sources contributing to chlorophenol in industrial effluents are from leather finishing, paint and ink formulating, and paper industries.

#### 1-2 Adsorption

An increased awareness of the occurrence of phenol, p-chlorophenol (PCP), pesticides and other pollutants in natural water has led to the emergence of adsorption by activated carbon as one of the most effective methods of removing these chemicals from drinking and wastewaters.

Adsorption is a surface phenomenon that is defined as the increase in concentration of a particular component at the surface or interface between two phases. In any solid or liquid, atoms at the surface are subject to unbalanced forces of attraction normal to the surface plane. These forces are merely extensions of the forces acting within the body of the material and are ultimately responsible for the phenomenon of adsorption.

#### 1-3 Activation

Activation is a physical change wherein the surface of the carbon is tremendously increased by the removal of hydrocarbons from the carbon structure. The two most important steps are carbonization and

oxidation. Both methods involve a reaction with oxidizing gases of steam, air, and carbon dioxide at an elevated temperature, which causes an extensive burnoff of noncarbon impurities.

In the past, a large scale study has been done on the phenomenon of activated carbon adsorption in a phenol aqueous system. A homogeneous solid phase diffusion model has been used to predict the breakthrough curve for phenol adsorption. But, no known existing literature refers to the adsorption capacities of activated carbon in tapered fixed bed experiments. Therefore, this research is a preliminary study of the adsorption capacities of activated carbon in a tapered fixed bed, because some early studies done by Mathews have shown that tapered bed has better efficiency in adsorption (slower breakthrough point) compared to circular bed.

#### 1-4 Objectives of study

- 1) To establish adsorption isotherm for phenol at 25°C.
- 2) To assess the ability of an adsorption model in order to predict the adsorption rates for phenol aqueous system.
- 3) To compare the adsorption processes between a columnar and a tapered fixed bed.

The scope of this research consisted of:

- 1) Establishing adsorption equilibrium and kinetics of phenol,
- 2) Conducting adsorption equilibrium experiments for single solute at 25°C to obtain isotherm parameters, and
- 3) Conducting kinetic studies to determine adsorption rates and transport parameters.

## CHAPTER 2

### REVIEW OF RELATED LITERATURE

#### 2-1 Single Solute Adsorption Models

##### 2-1-1 Equilibrium Models

Several mathematical relationships have been developed to characterize the equilibrium distribution of solute between the solid and liquid phases.

An adsorption isotherm is an expression of equilibrium at a given temperature between equilibrium concentration,  $C_e$ , which is the amount of organic compound left in solution, and surface concentration,  $q_e$ , the amount of compound on the surface of the activated carbon.

Two linear models, the Langmuir isotherm and the Freundlich isotherm are most commonly used to describe the equilibrium condition. The Freundlich isotherm (Freundlich, 1926)

$$q_e = KC_e^n \quad (2.1)$$

was developed empirically and was based on the assumption that the adsorbent had a heterogeneous surface composed of different classes of adsorption sites. Despite this assumption, the Freundlich isotherm is often used as a means of data description. A plot of  $\log(q_e)$  versus  $\log(C_e)$  should yield a straight line and  $K$  and  $n$  are constants depending on the temperature and the solute used.

The Langmuir isotherm (Langmuir, 1918) was theoretically derived on the assumptions that the maximum adsorption is monolayer, the energy of adsorption is constant, and there is no migration of solute

in the plane of the surface.

The Langmuir isotherm is generally written as

$$q_e = \frac{QbC_e}{1 + bC_e} \quad (2.2)$$

where  $Q$  is the number of moles of solute adsorbed by per unit mass of adsorbent in forming a complete monolayer on the adsorbent. The constant,  $b$ , is related to the energy of enthalpy, of adsorption.

In the case of adsorption by activated carbon in an aqueous system, neither Freundlich nor Langmuir isotherms may describe the data satisfactorily over a wide range of concentrations. An empirical equation with three parameters that represents data over wide range has been proposed by several investigators. (Redlich and Peterson, 1959; Radke and Prausnitz, 1972; and Mathews and Weber, 1977). The equation is of the form

$$q_e = \frac{AC_e}{1 + bC_e^\beta} \quad \beta \leq 1 \quad (2.3)$$

At low concentrations, this three parameter equation becomes linear and when  $\beta = 1$  it becomes the Langmuir isotherm. At high concentrations, this equation becomes the Freundlich isotherm. In this research, the three parameter equation was selected to describe equilibrium adsorption.

The BET isotherm (Weber, 1972) assumed that several layers of adsorbate molecules form at the surface of the adsorbent and that the Langmuir equation applies to each layer. The BET isotherm reduces to

the Langmuir model when the limit of adsorption is a monolayer. The BET model equation is commonly written as follow:

$$q_e = \frac{ACX_m}{(C_s - C) [1 + (A - 1) C / C_s]} \quad (2.4)$$

where

$q_e$  = amount of the solute adsorbed per unit mass of adsorbent,

$C$  = concentration of the solute in solution at equilibrium,

$C_s$  = saturation concentration of the solute,

$X_m$  = amount of the solute adsorbed in forming a complete monolayer, and

$A$  = a constant to describe the energy of interaction.

#### 2-1-2 Batch Kinetic Models

The rate at which equilibrium is attained in an adsorption system is described in a kinetic model. The process kinetics which describes the rates at which molecules are transferred from solution to the surface of the carbon particles involves several sequential and parallel transport and reaction phenomena. For adsorption to occur, the following steps must take place:

- (1) Film transfer - The adsorbate passes through a film surrounding the adsorbent particle to the surface of the particle.
- (2) Pore diffusion - The adsorbate diffuses through the pore of the particle.
- (3) Surface diffusion - The adsorbate diffuses along the surface of the pore.

(4) Adsorption - The solute becomes attached to the surface of the pore, that is, to be adsorbed.

Figure 2.1 represents the overall rates of adsorption of solute onto granular particles.

Several models have been used frequently to describe the different combination of rate processes in adsorption systems. The following models tried to simplify the rate processes by making assumptions:

- (1) An effective or overall reaction rate expression (Thomas, 1944; Hiester and Vermeulen, 1952; Keinath and Weber, 1968).
- (2) A linear or quadratic driving force approximation for intraparticle diffusion (Glueckauf and Coates, 1947; Vermeulen, 1953; Vassilion and Dranoff, 1962; Hall et al. 1966; Cooney and Strusi, 1972; Hsieh et al. 1977).
- (3) Film transfer as the only rate controlling factor (Garipey and Zwiebel 1971; Zwiebel et al. 1972; Kyte, 1973; Keinath, 1977).

Weber and Rumer (1965) have proposed a model considering pore diffusion, cylindrical particle shape, and Langmuir isotherm for adsorption of benzenesulfonates on activated carbon. This was followed by a proposed similar model with this model having spherical particles Snoeyink and Weber (1968). Neretnieks (1976) presented and solved equations for surface and combined diffusion along with film transfer by using forms of the Freundlich and Langmuir isotherms.

Digiano and Weber (1973) considered film resistance, pore diffusion and the Langmuir isotherm in their infinite batch model to describe data for p-nitrophenol and 2,4-dinitrophenol with activated



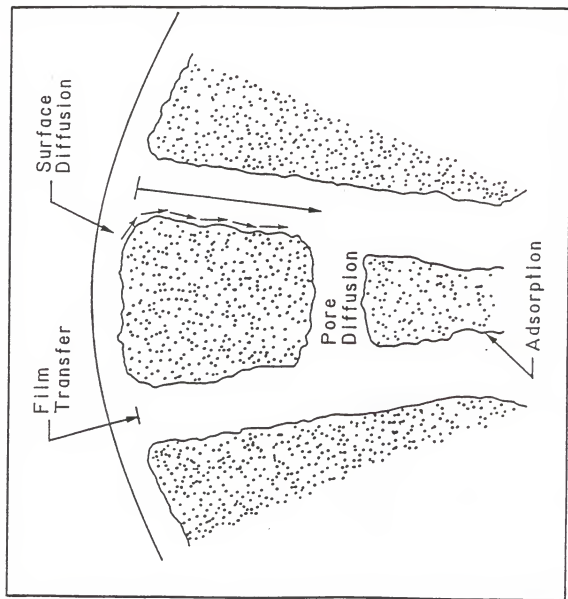


Figure 2.1 Adsorption on Porous Adsorbent ---  
Rate Limiting Mechanisms. (Lin, 1985)

carbon. The infinite batch system is one in which a boundary condition of concentration of solute in solution is implied. It was found that the anion forms of the solute did not diffuse as rapidly as in their neutral forms.

Rosen (1952) developed the homogeneous solid phase diffusion model to predict the adsorption rates in batch and fixed bed reactors. The model considered the film transfer and solid phase diffusion as the rate limiting steps and the model equations are solved numerically for the three parameter isotherm.

Mathews and Weber (1977) have successfully predicted adsorption for four solutes exhibiting widely different adsorption equilibrium and rate characteristics by using the homogeneous solid phases diffusion model with the three parameter isotherm.

The homogeneous solid phase diffusion model will be described in the next several paragraphs.

The concentration of the solute,  $C$ , and the distribution of the adsorbent particle may be assumed uniform throughout the rapidly agitated batch reactor. The film transfer from the fluid phase to the solid phase is expressed in terms of the time rate of change of the average solute concentration,  $q$ , of the particle.

$$\frac{dq}{dt} = \frac{k_f A_p}{V_p \rho} (C - C_s) \quad (2.5)$$

$k_f$  is the film transfer coefficient;  $A_p$ ,  $V_p$  and  $\rho$  are the surface area, volume, and density of the particle respectively;  $C$  is the concentration of the solute in the liquid expressed in moles/liter;

and  $C_s$  is the equilibrium liquid phase concentration at the particle surface.

The average solute concentration of the entire particle with a radius of  $R$  (cm) is obtained by integrating the pointwise concentration over the volume of the particles, yielding

$$q = \frac{3}{R^3} \int_0^R q r^2 dr \quad (2.6)$$

For a spherical particle, assuming symmetry in two directions, transport within the solid phase is given by

$$\frac{\delta q}{\delta t} = \frac{D_s}{r^2} \frac{\delta}{\delta r} \left( r^2 \frac{\delta q}{\delta r} \right) \quad (2.7)$$

$q$  is the dimensionless solid phase concentration at an internal radius,  $r$ , and  $D_s$  is the solid phase diffusion coefficient. The mass balance for the batch reactor is

$$V \frac{dC}{dt} = -w \frac{dq}{dt} \quad (2.8)$$

$V$  is the volume of solution, and  $w$  is the total weight of carbon. The initial boundary conditions are

$$@ t = 0 ; C = C_0 \quad (2.9)$$

$$@ t = 0, 0 \leq r \leq R : q = 0 \quad (2.10)$$

$$@ t \geq 0, r = 0 : \delta q / \delta r = 0 \quad (2.11)$$

$$@ t \geq 0, r = R$$

$$\frac{R^2 k_f}{\rho} (C - C_s) = \frac{\delta}{\delta t} \int_0^R q r^2 dr \quad (2.12)$$

$$@ r = R, C_s = f(q_s) \quad (2.13)$$

Equation 2.9 and 2.10 imply that the initial concentration of the solute in the liquid phase is  $C_0$  and zero in the solid phase.

Equation 2.11 shows that as time is greater than zero, the concentration gradient at the center of the particle is zero.

Substituting equation 2.6 into equation 2.5 gives equation 2.12; the mass balance on adsorbent particles. Equation 2.13 is the isotherm relations between surface concentration and solution concentration of solute. The three parameter equation, equation 2.3, is used to describe equilibrium,  $q_s$ , at the external surface.

Traegner and Suidan (1989) developed a parameter search procedure using the Levenberg-Marquardt numerical algorithm. This procedure uniquely determines the external film mass transfer and surface diffusion coefficients for the homogeneous surface diffusion model.

A technique for predicting granulated activated carbon (GAC) performance is developed by Clark et al. (1986). This technique used the freundlich isotherm and logistic function formulation and applied to the total organic carbon (TOC) loading. The results were verified by field study conducted in Cincinnati, Ohio.

Crittenden et al. (1987), proposed and verified correlations to determine single solute isotherm and mass transfer parameters. These correlations were used in combination with a simplified version of a mass transfer model to calculate mass transfer zone length and the

maximum amount of water that may be treated. The calculated results were used to select the optimum fixed-bed adsorber operation.

A mathematical model of simultaneous adsorption and biodegradation of a single substrate in beds of sorptive media is developed by Speitel et al. (1987). The model describes adsorption equilibrium and rate by Freundlich isotherm and surface diffusion respectively, whereas the biodegradation is described by Monod kinetics.

Mathews and Zayas (1989) used a Quantiment-720-23A programmable and computerized image analyzer to determine size and shape characteristics of individual carbon particles. Sauter mean of particle diameters from projected area measurements was recommended to account for the effects due to the variations in particle size and shape. Power-law correlations were developed to indicate the effect of batch adsorber parameters and particle size on the  $k_f$ .

### 2-1-3 Kinetics for Fixed Beds

A Number of models have been proposed using the rate processes as described above to predict the breakthrough profile of fixed beds.

Morton and Murril (1967) and Stuart and Camps (1973) used fixed bed models to describe surface and film diffusion. Colwell and Dranoff (1969) utilized the similar model but with axial dispersion. The experimental data fit both models well.

Wheeler and Middleman (1970) incorporated three types of resistances in their models. They were: intraparticle transport, surface reaction, and particle to fluid convective mass transfer.

Peel and Benedek (1980) developed a model accounting for the

internal structure of the activated carbon. This model proposed that the carbon particle has two regions; micropores and macropores. Rapid diffusion and adsorption takes place in macropores and the rest of it takes place in the micropores until equilibrium is reached. This model, however, did not show any improvement in prediction compared to other models.

Michigan Adsorption Design and Application Model (MADAM) was used by Weber and Pirbazari (1982) to simulate and predict the behavior of fixed beds in water treatment conditions.

Weber et al. (1987) used the MADAM to model the adsorption of target organic compounds in the presence of background dissolved organic matter. A bisolute version of MADAM sufficiently calibrated and predicted fixed-bed adsorber profiles for lindane and humic acid. A second modeling approach was used to investigate the adsorption equilibrium and rate parameters. The modeling was performed for a designated target compound (lindane) in the presence of a theoretically unspecified background water.

Snoeyink et al. (1986) discovered that the free or combined chlorine reacts with phenols adsorbed on GAC, and produced a series of oxidation products that were not formed in the absence of carbon. Products like p-benzoquinone, 2,4-dichlorophenol and 4,4'-dihydroxybiphenyl were strongly adsorbed and occupied adsorption sites causing premature breakthrough.

#### 2-1-4 Fixed Bed Model

Equation 2.7 and equations 2.9 to 2.13 from section 2-1-3 are

parts of the equations used to describe the fixed bed model. Other equations in the liquid phase conditions are as follow:

$$\frac{\delta C}{\delta t} + v \frac{\delta C}{\delta z} + \left( 3 \frac{1 - \epsilon_b}{\epsilon_b R} \right) k_f (C - C_s) = 0 \quad (2.14)$$

$$@ t = 0, 0 \leq z \leq L_b : C = 0 \quad (2.15)$$

$$@ t \geq 0, z = 0 : C = C_0 \quad (2.16)$$

Equation 2.14 gives the mass balance of the solute at any time in the bed. The first term is the rate of change in the concentration, the second term is the convective change in the concentration inside the bed, and the last term is the rate of mass transfer through the film to the solid surface. Here,  $v$  is the superficial liquid velocity,  $\epsilon_b$  is the porosity of the bed, and  $z$  is the bed height. In addition, equation 2.15 represents the initial condition of the bed at time equal to zero, whereas equation 2.16 shows that the solution concentration at the entrance to the bed is equal to the initial concentration at time equal to or greater than zero.  $L_b$  is the length of the bed, and  $C_0$  is the initial solution concentration.

#### 2-1-5 Solution of The Model

In the fixed bed model, the differential equations are solved by using the orthogonal collocation method which is one of several other weighted residual methods. In this method, the solution of the differential equations is approximated by trial and error having functions and/or constants. When this trial solution is substituted into the differential equation, the residual is forced to zero at collocation points. A special case of the collocation method is

orthogonal collocation, whereby the trial functions are a set of orthogonal polynomials and the collocation points are the roots of these polynomials. In orthogonal collocation, the partial differential equations are reduced to first order ordinary differential equations. These ordinary differential equations were then solved by a computer subroutine program developed by Gear (Gear, 1976; Hindmarsh, 1974). Later, Mathews and Kulkarni (1983) modified the program by treating the whole bed as a series of small beds of the same sizes containing one particular size of carbon.

The program was modified and equilibrium is represented by the three parameter isotherm. In the original program, single solute equilibrium constants were determined by fitting a Freundlich isotherm equation to the equilibrium data. Consequently, the curve portion of the data near low concentrations was represented by a linear isotherm resulted in erroneous predictions. There are several input data requirements to run the program:

- (1) weight of carbon,
- (2) bed height,
- (3) radius of adsorbent particle,
- (4) molecular weight of the solute,
- (5) influent concentration,
- (6) isotherm constants,
- (7) collocation constants,
- (8) intraparticle diffusion coefficient,  $D_s$  and
- (9) external mass transfer coefficient,  $k_f$ .

The  $D_s$  was established from batch studies and the sets of



equations suggested by Dwiwedi and Upadhyay (1977) to find  $k_f$  are as follows:

$$\epsilon J_d = 0.4548 N_{Re}^{-0.4069}, \quad N_{Re} > 10 \quad (2.17)$$

$$\epsilon J_d = 1.1068 N_{Re}^{-0.72}, \quad N_{Re} \leq 10 \quad (2.18)$$

$$J_d = (k_f/u) N_{sc}^{2/3} \quad (2.19)$$

where

$\epsilon$  = porosity of bed,

$J_d$  = mass transfer factor,

$N_{Re}$  = Reynolds number ( $D_p G / \mu$ ),

$D_p$  = particle diameter,

$G$  = superficial mass flow rate,

$\mu$  = absolute viscosity,

$u$  = superficial fluid velocity ( $G / \rho$ ),

$\rho$  = density,

$N_{sc}$  = Schmidt number ( $\mu / \rho D_L$ ), and

$D_L$  = molecular diffusivity.

Wilke and Chang (1955), developed an equation to calculate  $D_L$ :

$$D_L = T \times 10^{-7} (M)^{0.5} / (\mu v_o^{1/3}) \quad (2.20)$$

where

$T$  = absolute temperature in deg K,

$M$  = molecular weight of the solvent,

$\mu$  = solution viscosity in centipoise, and

$v_o$  = molal volume of the solute at normal boiling point.

\* refer appendix for sample calculation.

The ideal adsorbed solution (IAS) model was used by Kong and Digiano (1986) to predict multicomponent adsorption equilibria for carbon tetrachloride, trichlorethylene, and tetrachloroethylene in two component and three-component solution on activated carbon and carbonaceous resin. Single solute adsorption experiments were performed to acquire isotherm parameters and multicomponent adsorption experiments to verify IAS model results. The model described some of the multicomponent adsorption equilibria for the concentration range of 1-2000  $\mu\text{g/L}$ . However there were notable exceptions not easily explained by experimental error, suggesting that the IAS model may not be valid in general. It was concluded that carbonaceous resin had a higher capacity for each of the three volatile organic chemical than does activated carbon.

Later in 1987, Crittenden et al. developed an equilibrium column model (ECM) to evaluate multicomponent competition in fixed-bed adsorptions columns. The model ignored mass transfer resistances and used IAS theory to predict the competitive effects in multicomponent mixtures. ECM was shown to be able to calculate the elution order of the adsorbates, the lowest carbon usage rate in multicomponent mixtures, and the highest possible effluent concentrations due to competitive adsorption.

A rapid small scale column test (RSSCT) that uses a smaller adsorbent particle was used by Crittenden et al. (1987) to simulate a five-month pilot plant adsorption study in several days. The mathematical model includes the use of axial dispersion, intraparticle pore and surface diffusion. Liquid-phase mass transfer resistance is

used to scale down the RSSCT from the pilot plant operation without extensive isotherm and kinetic data. This study presented evidence that the surface diffusivities were not necessarily constant with adsorbent particle radius.

In the same year, Crittenden et al. (1987) proposed a hypothetical component classification procedure (HCCP) to predict fixed-bed removal of individual components of total surrogates such as total organic halogen (TOX) in mixtures of unknown composition.

Wilmanski and Lipinski (1989) modified the irreversible, one-component adsorption model to simulate the fixed-bed total organic carbon (TOC) removal. The model assumed that the pore diffusion coefficient was not constant.

Biodegradation of synthetic organic chemicals in GAC columns, may extend the GAC service life through in-situ biological regeneration of sorption sites by decreasing the chemical loading onto the GAC (Speitel et al. 1989). Biodegradation of p-nitrophenol (PNP), 2,4-dichlorophenol (DCP), and pentachlorophenol (PCP) were investigated over the concentration range of 1-25  $\mu\text{g/L}$ . PNP and DCP were found to be readily biodegraded but PCP biodegraded at a slower rate.

#### 2-1-6 Single Solute Fixed Bed With Two Or More Adsorbents

Numerous researchers have tried to correlate kinetics with different pore size distributions and surface areas. Smith et al. (1959) studied the adsorption of 2,4-dichlorophenol with four different types of activated carbon. It was found that there is a relationship between adsorption rate and micropores with less than

$2.50 \times 10^{-6}$  cm radius.

Westmark (1975) proposed a model with four different carbon sizes. The water used was treated by sedimentation, biological oxidation, coagulation with alum, and finally filtered to remove suspended particles. The contaminants were measured in terms of COD. By varying the values of the isotherm constants in the linear isotherms and pore diffusion, the experimental data was corrected for extremely adsorbable and nonadsorbable compounds.

Holzel et al. (1979) concluded that the p-nitrophenol exhibited a higher diffusivity in carbon with larger pore volume.

Lee et al. (1980) proposed a model to predict adsorption of humic substances on different carbons. By using film transfer coefficients and surface diffusivities independent of fixed bed experimental data, the model predicted the performance of the fixed bed very well.

## CHAPTER 3

### EXPERIMENTAL MATERIALS AND METHODS

#### 3-1 Materials

##### 3-1-1 Adsorbent

The adsorbent used in this research was granular activated carbon (Carborundum) supplied by CECA Inc., Pryor, Oklahoma. The properties of the carbon used are listed in Table 3.1.

The carbon is received from the manufacturer as No. 12/40 (particles passing through a U.S. Standard Mesh Size No. 12 screen but retained on No. 40 screen). For batch kinetic and equilibrium studies No. 25/30 and No. 30/35 were used respectively. In fixed and tapered bed experiments carbon No. 12/14, 14/16, 16/18 and 18/20 were used instead. The geometric mean diameter of a particle used in this research was calculated by  $(d_1 * d_2)^{1/2}$  where  $d_1$  is the mesh size of the upper sieve and  $d_2$  is the mesh size of the lower sieve (Table 3.2). The carbon was washed several times with tap water passing through carbon column before performing the experiments to remove fines and any foreign objects. The carbon was then dried to a constant weight in an oven at 200°C and kept at room temperature in airtight glass containers.

##### 3-1-2 Adsorbate

The solute used in the study was phenol. The properties of phenol are shown in Table 3.3. The solute was supplied by J.T. Baker Chemical Co. Phillipsburg, NJ. in crystal form stored in a dark glass bottle.

Table 3.1 Properties of the adsorbent.

---

Manufacturer	CECA Inc., Pryor, Oklahoma
U.S. Mesh size	12/40
Raw material	Bituminous coal
 Physical Properties -----	
Surface area, $\text{m}^2/\text{gm}$	1000-1100
Apparent density, $\text{gm/cc}$	0.47
Particle density wetted in water, $\text{gms/cc}$	0.60
Effective size, $\text{mm}$	1.9 or less

---

Table 3.2 Carbon size fraction and diameters.

Size fraction	Geometric mean diameter (microns)
#12-#14	1539
#14-#16	1290
#16-#18	1091
#18-#20	917
#20-#25	772
#25-#30	647
#30-#35	543

Table 3.3 Solute and its properties

Phenol	
Supplier	J.T. Baker Chemical Company
Reagent grade	Baker TM
Formula	$C_6H_5OH$
Molecular Weight	94.11
pKa	9.90
Melting point	43°C
Boiling point	181.75°C
Diffusivity in water @ 25°C (cm <sup>2</sup> /sec)	$10.43 \times 10^{-6}$



All stock solutions were prepared with tap water passing through a three foot carbon column to remove organic compounds from the water. This organic free water was used for batch studies, equilibrium studies, and fixed and tapered bed experiments. The temperature of the solute for all the experiments in this research was kept constant at 25°C while the pH was kept at 7.

### 3-2 Methods

#### 3-2-1 Analytical Methods

The concentrations of phenol solution were analyzed by ultraviolet light adsorption spectrophotometry with a Bausch and Lomb Spectronic 710 Spectrophotometer. A preliminary test was required to determine the wavelengths of maximum absorbance for phenol. Several different concentrations of phenol solutions were used to obtain the calibration charts independently at its wavelength of maximum absorbance. Phenol was analyzed at 270 nm with molar absorptivities  $\epsilon$  of 1466 /mole-cm which was determined from the slope of the calibration curves. The suitable absorbance (A) range for 10 mm photocell is  $0.1 \leq A \leq 1.2$ . A 50 mm photocell was used for low concentration samples (less than  $10^{-4}$  moles/L).

Friedel (1951) developed a relationship between the concentration of phenol,  $C_p$  (moles/L), absorbance, A,  $\epsilon$  and photocell size L (cm) which indicate:

$$C_p = \frac{A_{270}}{\epsilon L} \quad (3.1)$$

The concentration of phenol can then be determined knowing absorbance

at wavelength 270 nm and cell size.

### 3-2-2 Batch Kinetic Experiments

Batch kinetic experiments were conducted in a rectangular Plexiglas vessel with an internal dimension LxBxH of 34x30x35 cm. The schematic of the set-up is illustrated in Figure 3.1. A steel impeller was located at the center of the vessel and 7 cm from the bottom. A heater and a temperature regulator were used to keep the solution constant at 25°C.

Twenty-four liters of phenol solution with a concentration of  $2.5 \times 10^{-4}$  moles/L were introduced into the vessel with the solution kept at pH 7. No crystals of solute were introduced directly into the vessel. The impeller was maintained at a speed of 700 rpm to agitate the solution to reach equilibrium uniformly within the vessel.

After establishing this condition, samples were withdrawn to determine the initial concentration of the solution. At time  $t = 0$ , 6 gms of no. 25/30 carbon were added abruptly into the reaction vessel and agitated by the stirrer rapidly.

A glass tubing with a brass mesh wire attached to an end was lowered into the vessel during sampling. At a selected time interval, a sample of 10 ml was collected by inserting a pipette into the glass tubing. This was to prevent any carbon being drawn out of the vessel.

The sample collected for analysis resulted in a small decrease in the total adsorbate available to the adsorbent. Correction for this error was not required since the maximum cumulative error was not significant.

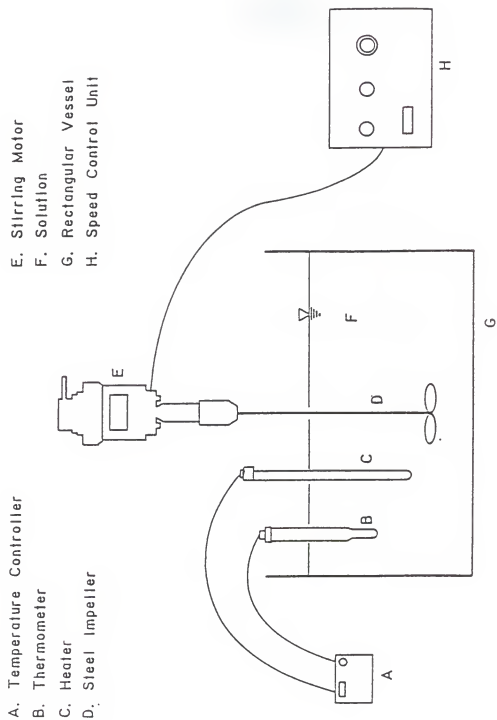
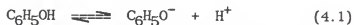


Figure 3.1 Schematic of Batch Kinetic System. (Lin, 1985)

The objective of these studies was to determine the  $D_s$ , solid phase diffusion coefficient and  $k_f$ , film transfer coefficient. Rate studies were conducted for carbon size 25/30, stirring speed of 700 RPM, reaction volume of 24 liters and total carbon weight of 6 gm. The initial concentration of phenol was  $2.5 \times 10^{-4}$  M and the pH was kept constant at 7 so that the solution would contain almost 100 % phenol.



By adding acid to the equilibrium equation 4.1, the reaction will shift to the left. A computer program written by Mathews (1975) was used to estimate the  $D_s$  and  $k_f$ . The input data necessary to run this program includes:

- (1) the three parameters isotherm A, B, and  $\beta$  from equilibrium studies,
- (2) weighted geometric mean diameter of the carbon used, and
- (3) initial estimate for  $k_f$  and  $D_s$ .

The film transfer coefficient can be calculated from batch data using equation 4.2.

$$k_f = \frac{-\ln (C_e/C_o) R \rho v}{t \quad 3w} \quad (4.2)$$

where

$C_e$  = concentration of solution at a specific time

$C_o$  = initial concentration of the solution

$t$  = time (sec.)

$R, \rho, w$  = radius, density and weight of carbon particle

respectively

$v$  = volume of solution

A graph of  $-\ln (C_e/C_0)$  versus  $t$  was plotted and the linear portion of the time points was fitted with a straight line. The value of  $k_f$  was then calculated from the slope. At a longer contact time, an increasing influence of intraparticle resistance causes nonlinearity.

### 3-2-3 Equilibrium Experiments

Equilibrium experiments were conducted by the standard bottle-point method to investigate the capacity of carbon at various solution concentrations. This method allows a solution with known initial concentration to come into contact with different amounts of carbon dosages until equilibrium is reached. The carbon used for these experiments was No. 30/35. The water used in making the standard solution was boiled in order to kill the microorganisms present in the water. This is to eliminate any interactions of the microorganisms with the teflon cap of the bottles.

Different carbon dosages varying from 0.1 to 1.0 gm were added into a series of 250 ml glass bottles (washed and dried) which contained 100 ml of phenol with known initial concentration.

Once the solutions and the carbon were introduced into the bottles, the bottles were sealed with teflon caps to ensure airtightness and placed in a Controlled Environment Incubator Shaker (Lab-line Instruments Inc.), with the temperature set at 25 °C. The shaker was manipulated in such a way that the carbon particles were always kept suspended and not stuck to the sides of the bottles. One

bottle consisting of only solution (without carbon) was set aside as a control to determine if the glass or teflon cap adsorbed any of the solutes. In addition, there were three bottles with the same amount of carbon dosages to ensure that equilibrium was reached. The maximum absorbance was reached on the eighth day. After equilibrium was reached, the samples were then analyzed for their final concentration.

The amount of solute adsorbed per unit mass of carbon,  $q_e$  was then determined by

$$q_e = (C_0 - C_e) V / W \quad (3.2)$$

where

$q_e$  = surface concentration (mmoles/gm)

$C_0$  = initial concentration of solutes (moles/l)

$C_e$  = final concentration of solutes (mmoles/l)

$V$  = volume of solutes (liters)

$W$  = weight of carbon (gm)

By using different amounts of carbon dosages, an isotherm profile can be determined and plotted on a log-log scale since each bottle represents a point on the equilibrium curve.

The three parameter equation correlates equilibrium relation between surface concentration,  $q_e$ , and solution concentration,  $C_e$ .

$$q_e = \frac{AC_e}{1 + BC_e^\beta} \quad \beta \leq 1 \quad (2.3)$$

A, B, and  $\beta$  are determined by the best statistical representation of the experimental data and estimated by a nonlinear parameter estimation

technique developed by Mathews (1975).

### 3-2-4 Fixed Bed Experiments

Figure 3-2 shows the schematic of the fixed bed experiment. The fixed bed was a glass column with an inner diameter of 5.08 cm and a height of 30 cm. In this research, all experiments were conducted with downflow. The carbon in the column was supported by a brass wire at one end. Table 3.4 outlines the operating conditions for the fixed bed.

A 30-gallon tank in which a constant head was maintained by overflow, supplied a continuous flow for the experiments. The water collected in this tank was produced by passing tap water through a three-foot long carbon column. This was to remove organic and other adsorbate from the tap water. Two variable flow pumps were manipulated to force the water, as well as the concentrated solution, into the fixed bed column at a combined flowrate of 830 ml/min. Flow meters were used to monitor the flow rate of the concentrated solution and solution entering the column at 30 and 830 ml/min respectively. The concentrated solution was stored in a 40-liter jar and maintained at a higher concentration than that required in the experiments. The flow from the jar was adjusted to have proper dilution to the desired concentration in the system. Constant checks on this influent concentration were required to ensure a minimum variation in flowrate.

A predetermined amount of carbon was introduced into the column. In case a mixture of sizes was used, the smallest size was introduced first, followed by the next larger size, and so on. In this

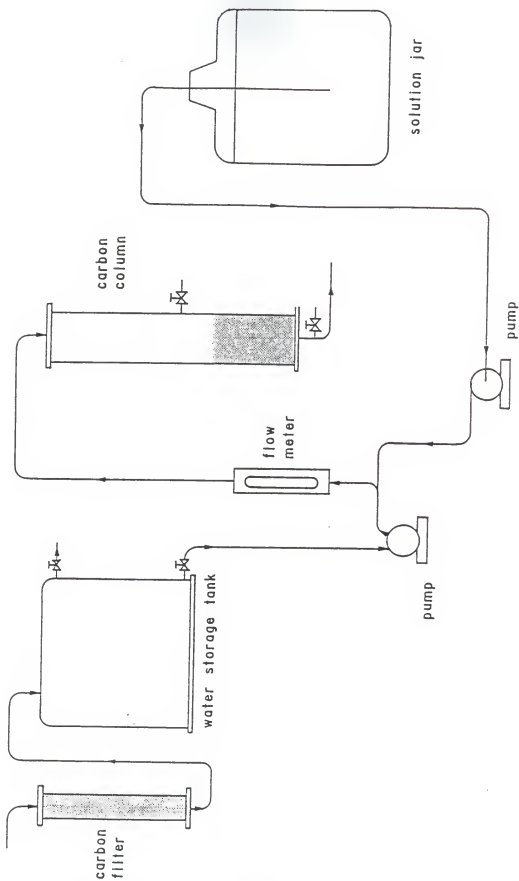


Figure 3.2 Schematic of Fixed Bed Adsorption System . (Lin, 1985)



Table 3.4 Fixed bed operating conditions.

Sieve Size fraction	Column diameter (cm)	Flowrate (ml/min)	Hydraulic loading rate (m/min)
#12-#14	5.08	830	0.4095
#14-#16	5.08	830	0.4095
#16-#18	5.08	830	0.4095
#18-#20	5.08	830	0.4095
mixed sizes (12/14, 14/16, 16/18 and 18/20)	5.08	830	0.4095

experiment, equal dosages of carbon No. 12/14, 14/16, 16/18 and 18/20 were used as mixed sizes. Carbon 12/14 would come into contact with the solution entering the column first and carbon No. 18/20 would be the last carbon size that the solution flowed through before it flowed out of the column. A few modifications were needed before the prediction model for mixed sizes could be run.

The first method was to use the average diameters of the mixed carbon sizes as an input data. Then, using the equation by Upadhyay and Dwiwedi (1977), the film transfer coefficient was determined. Surface diffusion coefficient was resolved by taking the mean of the coefficient of the individual carbon sizes which were established from batch studies with single sized particles.

The second method was to treat the different carbon sizes as separate individual layers. In this experiment, four values of the film transfer and surface diffusion coefficient were needed since there were four layers of carbon used.

Another fixed bed experiment was set up the same as the one described above (mixed sizes), but the order of the carbon in the column was reversed.

Water was passed through the column before the start of the experiment for about 15 minutes and the walls of the column were gently tapped to remove all the entrapped air.

Before the column could be operated, the temperature in the constant head tank was maintained at a higher temperature using a heater and a temperature regulator. When this water mixed with the solution from the jar, the temperature of the combined solution was

exactly 25°C. Once again, the pH of the solution entering the column needed to be 7.

The procedure adopted for maintaining the pH of the solution entering the column equal to 7 is described below:

Let  $T$  (ml) = volume of acid needed in the 40 liters solution jar to maintained pH = 7

$Q$  (ml) = total amount of acid needed in the solution jar to bring down the pH of the solution entering the column to 7

$$T \times 830 / 30 = Q \quad (3.3)$$

A mass balance equation was used to determine the concentration of the solution in the jar.

$$F_1 C_1 + F_2 C_2 = F_3 C_3 \quad (3.4)$$

where

$F_1, F_2, F_3$  = flowrate of water, solution in the jar, and solution entering the column respectively.

$C_1, C_2, C_3$  = concentration of water (taken as zero), solution in the jar and solution entering the column respectively.

As  $C_3$  ( $10^{-3}$  moles/l, in this experiments) and  $F_3$  (830 ml/min) are known,  $C_2$  can be determined from Equation 3.4.

The column was operated until the ratio of effluent concentration,  $C_e$ , to influent concentration,  $C_o$ , reached 0.90. The duration of the experiment was usually 14 hours. Effluent solutions were sampled at

intervals of an hour and were analyzed for concentration. Breakthrough curves were hence obtained by plotting  $C_e/C_0$  against time.

### 3-2-5 Tapered Bed Experiments

All the procedures and methods outlined for the fixed columnar bed applied for the tapered bed experiments.

Predetermined amounts of carbon were first filled up at the smaller end of the tapered bed and the remaining empty spaces were then occupied by glass balls and glass marbles. The experiments were set up for downflows. The influent solution comes into contact with the carbon through the narrower end and flows out through the wider end (Figure 3.3).

The tapered bed was made from plexiglas and stands at a height of 71 cm. The top rectangular segment measured  $2.54 \text{ cm}^2$  by  $10.7 \text{ cm}^2$  tall, which was filled up with glass balls measuring 3 mm in diameter. The function of this segment was to act as a distributor. The bottom section of the tapered bed measured  $2.54 \text{ cm}^2$  and widened to  $9.5 \text{ cm}^2$ . A brass wire mesh separated the glass ball from the carbon (Figure 3.4).

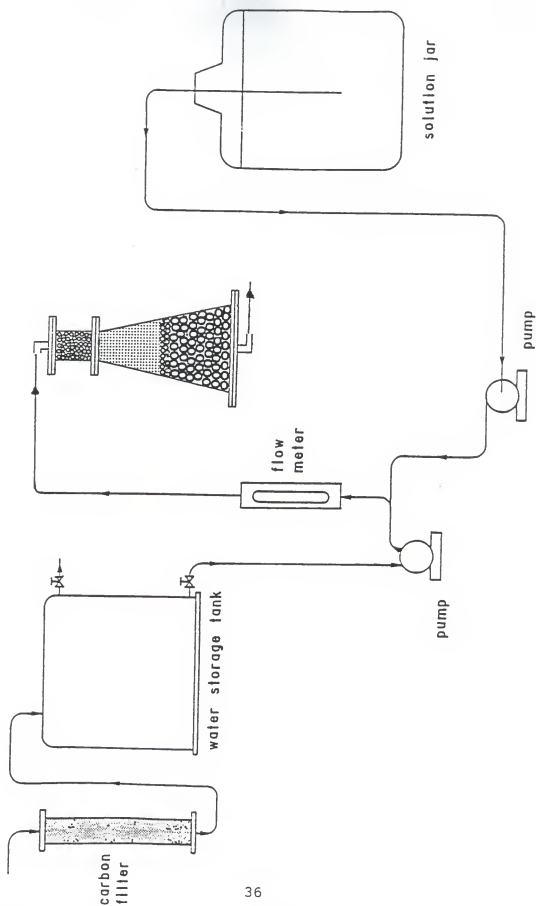


Fig. 3.3. Schematic of tapered bed adsorption system. (units in cm.)

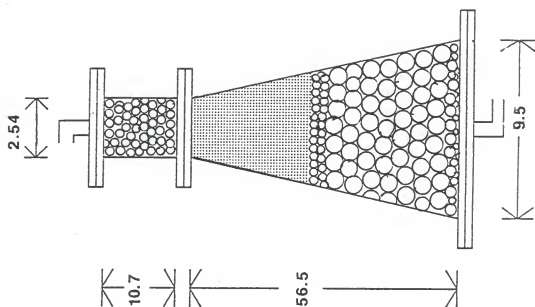


Fig. 3.4. Schematic of tapered bed. (units in cm.)

## CHAPTER 4

### RESULTS AND DISCUSSION

#### 4-1 Equilibrium Studies

Experimental results of surface concentration  $q_e$ , and solution concentration  $C_e$ , obtained in section 3-2-3 are fitted by equation 2-3 with parameter values summarized in Table 4.1. The corresponding data are plotted in Figure 4.1.

The adsorbate (phenol) removal per unit weight of carbon is nearly the same at all equilibrium concentrations along the isotherm plot due to the flat slope.

#### 4-2 Batch Kinetic Studies

Figure 4.2 gives the experimental and predicted plot for batch studies for phenol solution and size fraction 25/30. It shows that the experimental data is very close to the predicted value. The optimum contact time in Figure 4.2 is about 240 minutes. At the initial stage of the adsorption process in batch reactors, film diffusion is the rate limiting steps. As the carbon becomes loaded with the adsorbate, the reaction rate is then controlled by intraparticle diffusion.

Table 4.2 lists the sieve size used, where  $k_f$  and  $D_s$  are estimated from the batch rate data for phenol. It is noted that the  $k_f$  decreases as the particle size of carbon increases. On the other hand, the  $D_s$  is nearly independent of the carbon particle size.

Table 4.1 Three parameter isotherm constants for phenol.

Solute	A	B	$\beta$
phenol	15.11	7.546	0.8685

Source: Kunjupalu (1986)



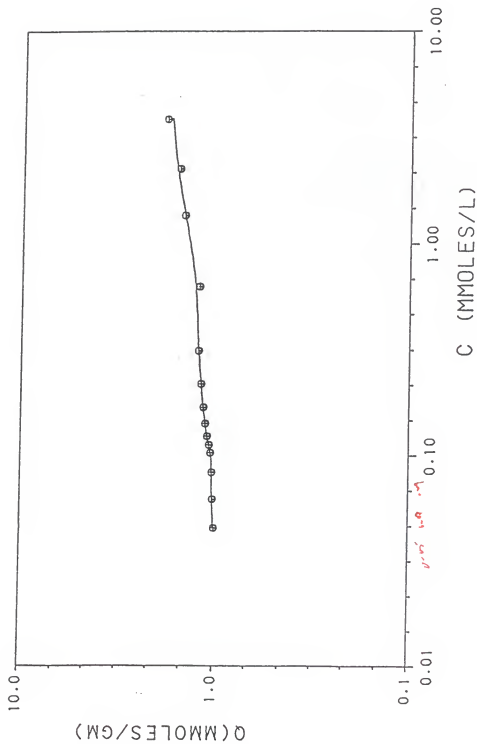


Fig. 4.1 Adsorption isotherm for phenol at 25°C.  
(  $\circ$  ) experimental data, ( — ) predicted values.

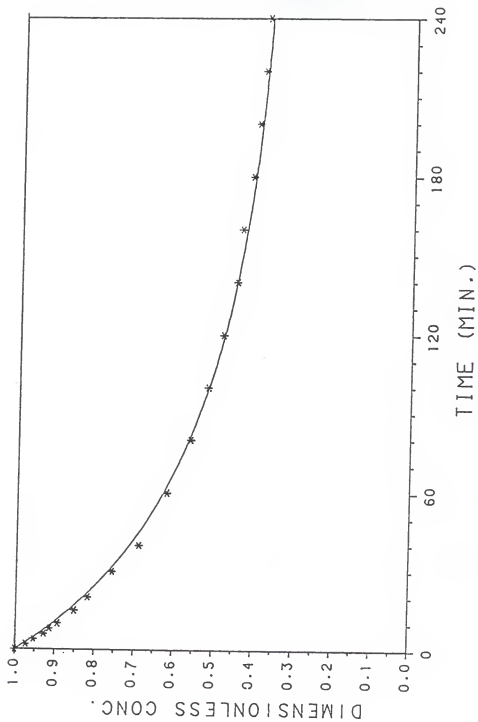


Fig. 4.2 . Adsorption rate for phenol for carbon size #25/30. ( \* ) experimental data. ( — ) prediction using geometric mean diameter.

Table 4.2 External fixed-bed mass transfer coefficients and intraparticle diffusion coefficient for phenol adsorption for single adsorbent sizes.

Size fraction	Geometric mean diameter (microns)	* $k_f$ (cm/s)* $10^3$	** $D_s$ (cm <sup>2</sup> /s)* $10^8$
#12-#14	1539	3.13	3.4
#14-#16	1290	4.11	3.3
#16-#18	1091	4.69	3.3
#18-#20	917	5.62	3.2
mixed sizes (#12/14, #14/16 #16/18 and #18/20)	1209	5.02	3.3

\* calculated from equations suggested by Dwiwedi and Upadhyay (1977), referes appendix for detail calculations. These values correspond to operating conditions shown in Table 4-4.

\*\* Kunjupalu (1986)

### 4-3 Single Solute Studies for Single Sizes.

#### 4-3-1 Column

The column studies were the fixed bed type and the column was operated in a downflow direction. Phenol was used as a solute in these experiments. The data collected in the column fixed bed experiments were applied to judge the efficiency of the mathematical model in predicting breakthrough curves. Table 4.3 illustrates the operating conditions for the column fixed bed in phenol adsorption.

As noted earlier, the rates of adsorption is controlled by transport processes at the surface of or within the carbon granule, and therefore depend greatly on the particle size of the adsorbent.

Figures 4.3 to 4.6 show the experimental and predicted breakthrough curves for phenol with single carbon sizes. The percent deviation of experimental to predicted results was within 5%. The "breakpoint" on these curves are those points at which the effluent from the adsorber no longer can adsorb the adsorbate satisfactorily. It can be seen from those figures that after a trace of solute was detected in the effluent, the concentration rose gradually at first and then sharply until it approached the value of influent concentration.

The general pattern of breakthrough curves has a characteristic S shape. Factors which affect the actual shape of the breakthrough curve include pH, rate-limiting mechanisms, adsorbate concentration, particle size of the adsorbent, depth of the column or bed, and the velocity of fluid. In general, the time to reach breakthrough for a specific type of adsorbent and a given adsorbate is decreased by:

increased particle size of the adsorbent, increased concentration of adsorbate in solution, increased flow rate, and decreased bed depth.

From Figures 4.3 to 4.6, it can be concluded that carbon size #18/20 has the slowest breakthrough of about six hours.

#### 4-3-2 Tapered Bed

The operating conditions for the tapered bed were the same as for the circular bed. Figures 4.7 and 4.8 present the predicted and experimental breakthrough curves for carbon sizes #12/14 and #16/18. At  $C/C_0 = 0.05$  and  $0.1$  for carbon size #12/14, the improvement in slowing the breakthrough time by the tapered bed was 62% and 38% respectively. Similarly at the same  $C/C_0$ , the improvement for carbon #16/18 was 24% and 17% respectively. Eventhough these results clearly demonstrated that the tapered bed operated at a better efficiency than the circular bed, more details studies like optimum angle of taper and studies on channeling effects in the tapered bed need to be done, before the results can be conclusive.

#### 4-4 Single Solute Studies for Mixture of Carbon Sizes

##### 4-4-1 Column

A mixture of carbon sizes were also used in the column studies. Table 4.4 gives the operating conditions for phenol adsorption for a mixture of sizes. Figure 4.9 shows that the tapered bed has slower breakthrough curve than the circular bed. An elaborate discussion can be found in section 4-4-3.

There were less than 5% deviation between the breakthrough curves using average diameter method and the stratified layer method, Figure 4.10.

Table 4.3 Fixed bed operating conditions for single size.

Sieve Size fraction	Column diameter (cm)	Flowrate (ml/min)	Hydraulic loading rate (m/min)	Weight of carbon (gms)
#12-#14	5.08	830	0.4095	250
#14-#16	5.08	830	0.4095	250
#16-#18	5.08	830	0.4095	250
#18-#20	5.08	830	0.4095	250

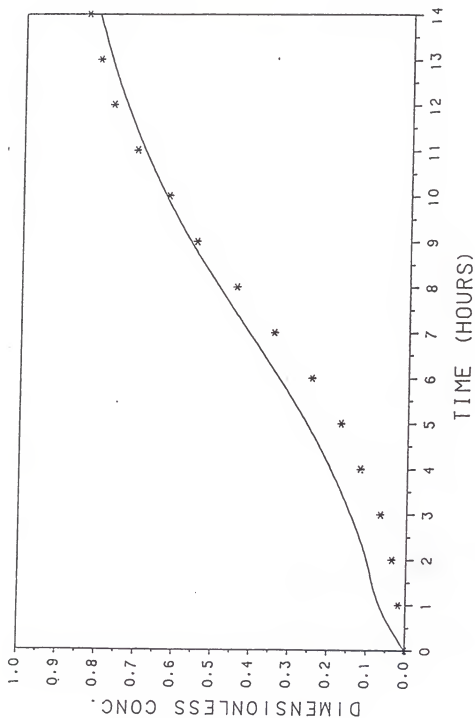


Fig. 4.3 . Breakthrough curve for phenol adsorption in circular column for carbon size #12/14. ( \* ) experimental data. ( — ) prediction using geometric mean diameter.

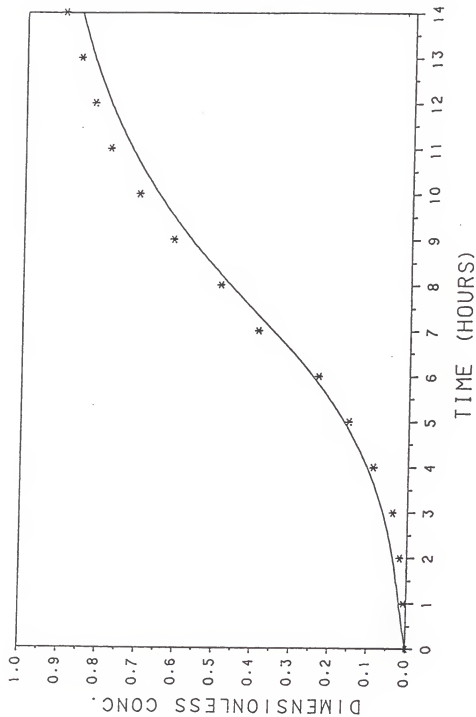


Fig. 4.4 . Breakthrough curve for phenol adsorption in circular column for carbon size #14/16. ( \* ) experimental data. ( — ) prediction using geometric mean diameter.



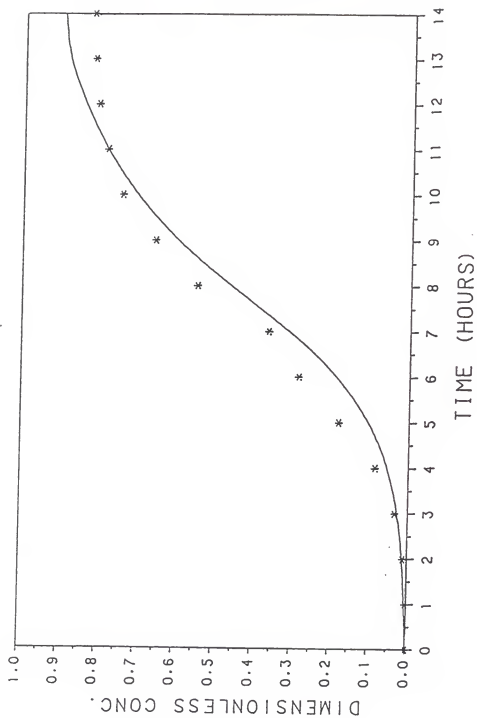


Fig. 4.5 . Breakthrough curve for phenol adsorption in circular column for carbon size #16/18. ( \* ) experimental data. ( — ) prediction using geometric mean diameter.

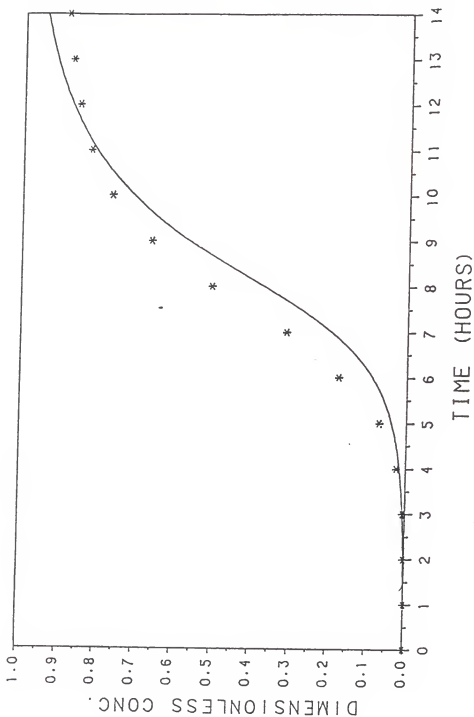


Fig. 4.6 . Breakthrough curve for phenol adsorption in circular column for carbon size #18/20. ( \* ) experimental data. ( — ) prediction using geometric mean diameter.

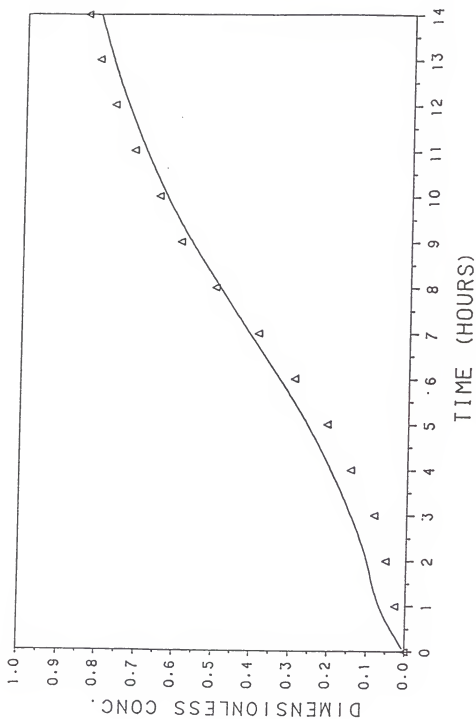


Fig. 4.7 . Breakthrough curve for phenol adsorption for carbon size #12/14. ( $\Delta$ ) experimental data for tapered bed. (—) prediction for circular column.

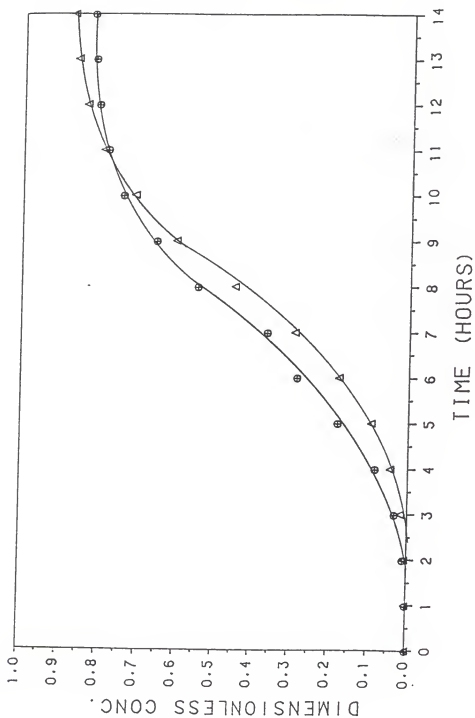


Fig. 4.8 . Breakthrough curve for phenol adsorption for carbon size #16/18. ( $\Delta$ ) experimental data for tapered bed. ( $\circ$ ) experimental data for circular column.

Table 4.4 Fixed bed operating conditions for mixed sizes.

Sieve Size fraction	Column diameter (cm)	Flowrate (ml/min)	Hydraulic loading rate (m/min)	Weight of carbon (gms)
#12-#14	5.08	830	0.4095	250
#14-#16	5.08	830	0.4095	250
#16-#18	5.08	830	0.4095	250
#18-#20	5.08	830	0.4095	250
mixed sizes (12/14, 14/16, 16/18 and 18/20)	5.08	830	0.4095	62.5 (each size)

Figure 4.11 exhibits the fact that even when the carbon layers in the column was reversed (#18/20, #16/18, #14/16 and #12/14), the model still predicted the experimental data well; there is less than 5% deviation between the experimental data and the predicted value. The sudden fluctuation of concentration at the end of the experiment might be due to non uniform flowrate at that moment.

#### 4-4-2 Sensitivity analyses

Sensitivity analyses were performed on the column studies for the mixed sizes. Figures 4.12 to 4.15 reveal that if  $k_f$  is decreased from  $5.08 \times 10^{-3}$  to  $2.54 \times 10^{-3}$  ( $0.5k_f$ ) and  $1.52 \times 10^{-3}$  ( $0.3k_f$ ) the prediction is far off the experimental values. In this case, both the  $0.5k_f$  and  $0.3k_f$  have faster breakthrough, but the former is slower than the latter. This is because with the same flowrate, as  $k_f$  increased there is little change in the breakthrough curve. However at a lower value of  $k_f$  the system is essentially intraparticle, and film transfer coefficient will be the controlling factor. Conversely if  $k_f$  increases, the solid phase diffusion coefficient takes over as the limiting factor in the model.

#### 4-4-3 Tapered Bed

Tapered bed was again used in comparison to circular bed in phenol adsorption for a mixture of carbon sizes. Under the same operating conditions, Figure 4.9 provides evidence that the tapered bed has a slower breakthrough than the circular bed.

At  $C/C_0 = 0.05$  and  $0.1$ , the improvement of the tapered bed over the circular bed was 19% and 18% respectively.

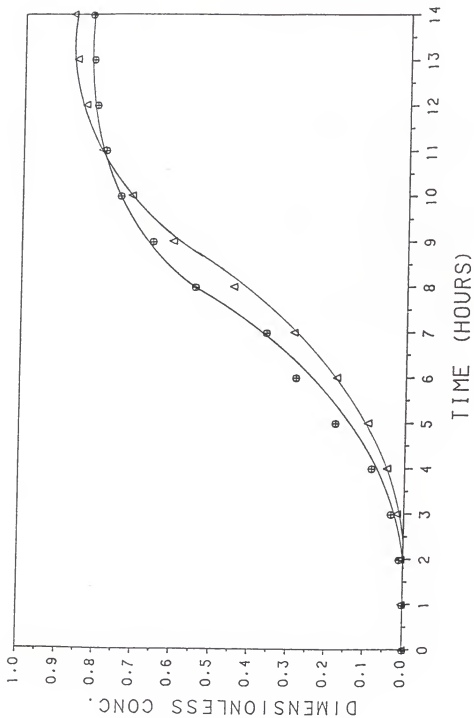


Fig. 4.9 . Breakthrough curve for phenol adsorption for carbon mixed size #12/14, #14/16, #16/18, and #18/20. (—○—) experimental data for circular column. (—△—) experimental data for tapered bed.

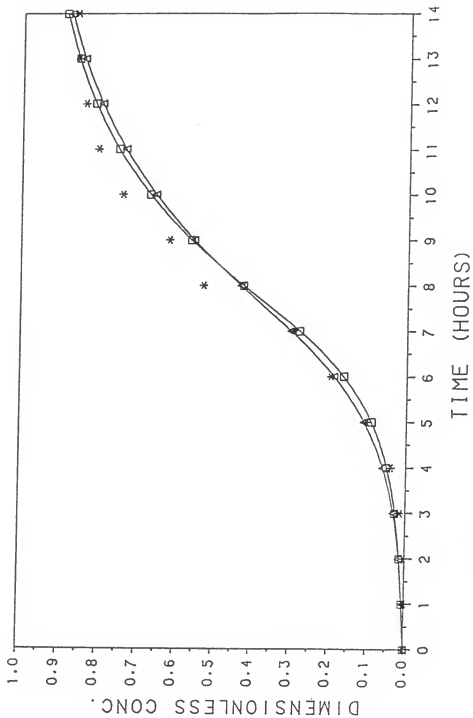


Fig. 4.10 . Breakthrough curve for phenol adsorption in circular column for carbon mixed size #12/14, #14/16, #16/18 and #18/20. ( \* ) experimental data. (—□—) prediction using average diameter. (—□—) prediction by layer.



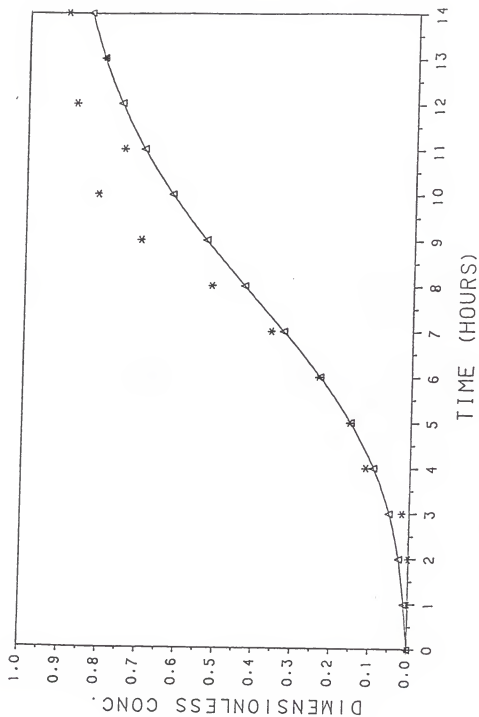


Fig. 4.11 . Breakthrough curve for phenol adsorption in circular column for carbon reversed mixed size #18/20, #16/18, #14/16 and #12/14. ( \* ) experimental data. (  $\Delta$  ) prediction by layer.

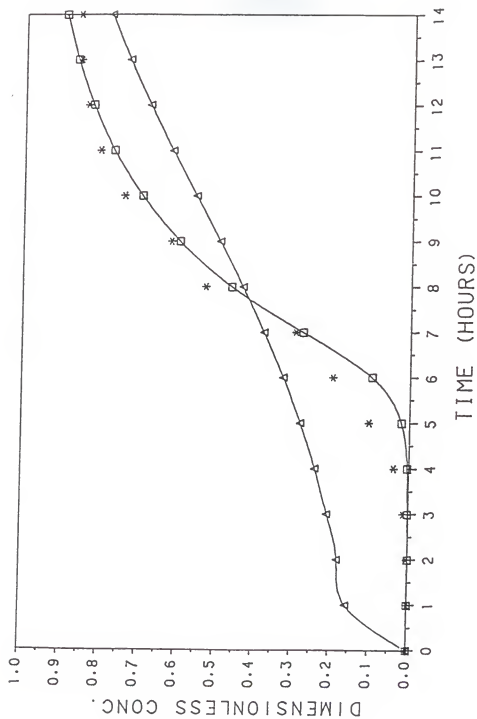


Fig. 4.12. Breakthrough curve for phenol adsorption in circular column for carbon mixed size #12/14, #14/16, #16/18 and #18/20. (\*) experimental data. (△) prediction with  $0.3k_f$ . (□) prediction with  $3k_f$  using average diameter.

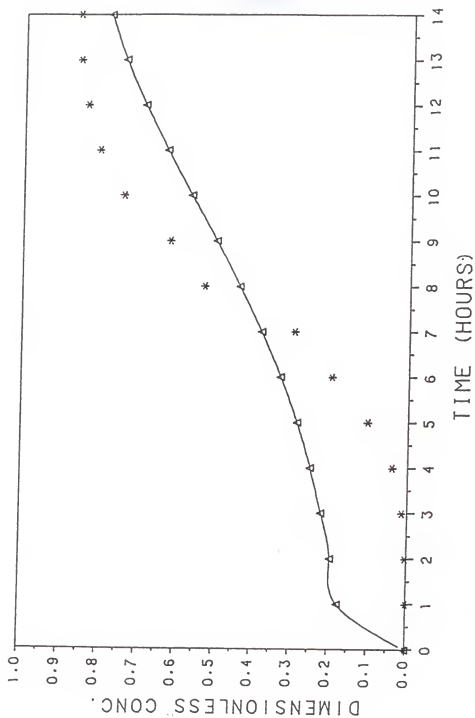


Fig. 4.13. Breakthrough curve for phenol adsorption in circular column for carbon mixed size #12/14, #14/16, #16/18 and #18/20. (  $*$  ) experimental data. (  $\Delta$  ) prediction by layer with  $0.3k_f$ .

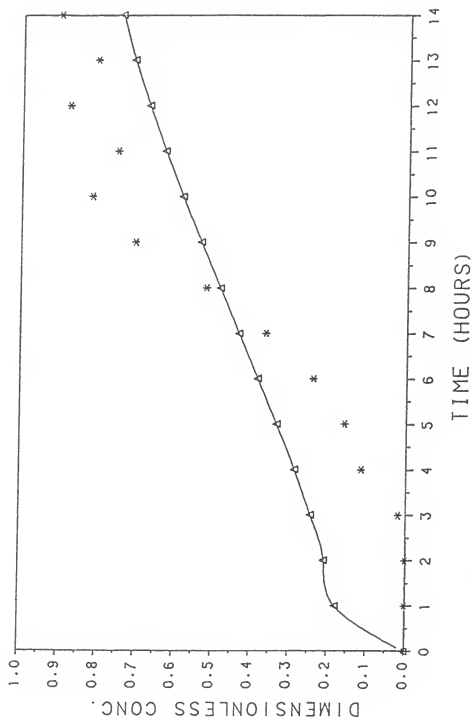


Fig. 4.14. Breakthrough curve for phenol adsorption in circular column for carbon reversed mixed size #18/20, #16/18, #14/16, #12/14. (\* ) experimental data. ( Δ ) prediction by layer with 0.3k<sub>f</sub>.

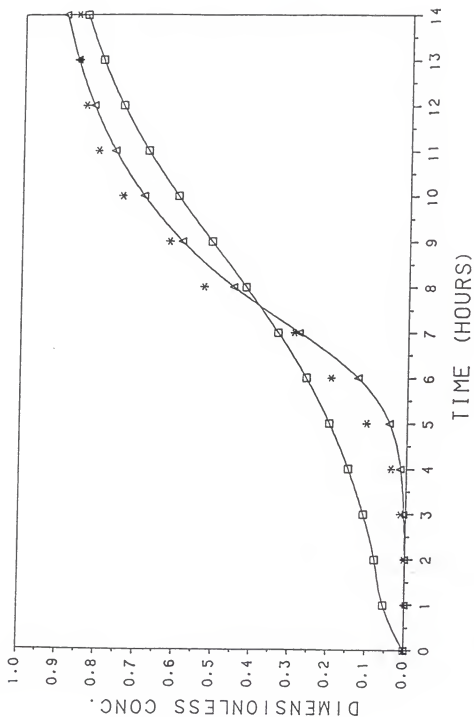


Fig. 4.15 . Breakthrough curve for phenol adsorption in circular column for carbon mixed size #12/14, #14/16, #16/18 and #18/20. (\* ) experimental data. (—□—) prediction with  $0.5k_f$ . (—△—) prediction with  $2k_f$  using average diameter.

## CHAPTER 5

### SUMMARY AND CONCLUSIONS

#### 5-1 Summary and Conclusions

Equilibrium studies were conducted for the adsorption of phenol on activated carbon from water. The tests were conducted with tapwater passed through a carbon column and boiled to destroy microorganisms in the water. The temperature for the tests was 25°C, and the pH of the water was adjusted to 7. Eight days were required to attain equilibrium. The data were fitted by the three parameter isotherm equation which was established by Mathews and Weber (1977). It was seen that the three parameter isotherm fitted the experimental data well.

Batch studies were conducted for phenol for single adsorbent sizes. For all the experiments performed during batch studies, the pH of the water was maintained at 7 and the temperature was kept constant at 25°C.

For phenol adsorption in single sizes, the film transfer coefficient increased as particle size decreased to within the size range of 1539 microns to 917 microns. In addition, the surface diffusion coefficient was reasonably constant ranging from  $3.2 \times 10^{-8}$  to  $3.4 \times 10^{-8} \text{ cm}^2/\text{s}$  for the same size range. It was concluded that the prediction model agreed with the experimental data.

Fixed bed studies were conducted for single adsorbent sizes as well as for a mixture of adsorbent sizes. A 5.08 cm column was used for the carbon sizes #12/14, #14/16, #16/18, and #18/20. The

temperature and pH were maintained at 25°C and 7, respectively. The fixed bed program based on the homogeneous solid phase diffusion model which was modified by Mathews (1984) was used to predict breakthrough curves of phenol at 25°C.

For column studies, it was seen that in the case of single adsorbent sizes as well as for a mixture of adsorbent sizes fitted by average and by stratified layer methods, the percent deviation of experimental to predicted values was within 5% . Similarly, the deviation for reversed mixed sizes (#18/20, #16/18, #14/16, and #12/14) was also 5%.

The operating conditions in the tapered bed studies, were identical to the column studies. At  $C/C_0 = 0.05$  and 0.1 for carbon size #12/14, the improvement in delaying the breakthrough time by the tapered bed over the circular bed was 62% and 38% respectively. Similarly, at the same  $C/C_0$  as above, the improvement for carbon #16/18 was 24% and 17% respectively.

For the mixed sizes (#12/14, #14/16, #16/18 and #18/20), and at the same two  $C/C_0$  of 0.05 and 0.1, the improvement of tapered bed over circular bed was 19% and 18% respectively.

The above results for the tapered bed indicate that it operates at a better efficiency than the circular bed in both mixed and single sizes.

Prediction using the average diameter and layered methods did not show any significant deviation from each other.

Sensitivity analyses were conducted for the mixed sizes and the results indicated that with the same flowrate, as  $k_f$  (film transfer

coefficient) increased, there is little change in the breakthrough curve. However, at a lower values of  $k_f$ , the system is essentially intraparticle and film transfer coefficient will be the controlling factor. Conversely if  $k_f$  increases, the solid phase diffusion coefficient takes over as a limiting factor in the model.

## 5-2 Recommendations

- 1) Develop a model to predict breakthrough for a single or multisolute in the tapered bed.
- 2) Design and construct the tapered bed for optimum adsorption. Increase or decrease the existing tapered angle to attain optimum "break point". Care must be taken not to increase the tapered angle too much as the channeling effect will occur.



## APPENDIX

\*\*\*\*\*  
 Sample calculations for fixed-bed external mass transfer coefficient  
 using Dwiwedi and Upadhyay's (1977) equations.  
 \*\*\*\*\*

carbon #12/14

$$\begin{aligned} \text{volume of carbon} &= \text{mass of carbon} / \text{density of carbon} \\ (V_c) &= 250 / 0.672 \\ &= 372.024 \text{ cm}^3 \end{aligned}$$

$$\begin{aligned} \text{volume of bed} &= \text{cross sectional area of bed} \times \text{bed height} \\ (V_b) &= 20.268 \times 30.8 \\ &= 624.264 \text{ cm}^3 \end{aligned}$$

$$\begin{aligned} \text{porosity of bed} &= (V_b - V_c) / V_b \\ (\epsilon) &= 0.404 \end{aligned}$$

$$\begin{aligned} \text{superficial fluid velocity } u &= G / p = \text{flow rate} / \text{cross section of bed} \\ &= 830 / 20.268 \\ &= 40.951 \text{ cm/min} \\ &= 0.6825 \text{ cm/sec} \end{aligned}$$

$$\begin{aligned} G / p_{\text{solution}} &= 0.6825 \\ G &= 0.6825 \times 0.997 \\ &= 0.6805 \text{ g}/(\text{sec cm}^2) \end{aligned}$$

$$\begin{aligned} \text{Schmidt number } N_{sc} &= \mu / \rho D_L \\ &= 0.8904 \times 10^{-2} / (0.997 \times 10.43 \times 10^{-6}) \\ &= 856 \end{aligned}$$

$$\begin{aligned} \text{Reynolds number } N_{Re} &= D_p G / \mu \\ &= 0.1539 \times 0.6805 / (0.8904 \times 10^{-2}) \\ &= 11.76 \end{aligned}$$

$$\begin{aligned} \text{equation 2.17: } \epsilon J_d &= 0.4548 N_{Re}^{-0.4069} \cdot N_{Re} > 10 \\ J_d &= 0.4129 \end{aligned}$$

$$\begin{aligned} \text{equation 2.19: } J_d &= (k_f / u) N_{sc}^{2/3} \\ k_f / u &= 4.580 \times 10^{-3} \\ k_f &= 3.125 \times 10^{-3} \text{ cm/s} \end{aligned}$$

Calculated external mass transfer coefficient  $k_f$  for fixed bed model using Dwiwedi and Upadhyay's (1977) equations.

Sieve no.	Geo. mean dia. (cm)	Bed Ht. (cm)	Porosity of bed	Reynolds num.	Mass Tran. factor $J_d$	Film Transfer coef. $k_f$
12/14	0.1539	30.8	0.4041	11.76	0.4129	3.13E-03
14/16	0.1290	30.2	0.3922	9.86	0.5432	4.11E-03
16/18	0.1091	30.0	0.3882	8.34	0.6193	4.69E-03
18/20	0.0917	29.0	0.3671	7.01	0.7421	5.62E-03
Mixed sizes	0.1209	27.5	0.3325	9.24	0.6712	5.08E-03

Superficial Fluid Velocity  $u = 0.6825$  cm/sec

Schmidt Number = 856

Tapered Bed Operating Conditions.

*****		
Sieve no.	Bed Height (cm)	Bed Diameter (cm)
*****		
12/14	27	6
16/18	23.5	5.5
Mixed size	26.5	5.9

## REFERENCES

- Clark R. M., J. M. Symons, J. C. Ireland (1986). Evaluating Field Scale GAC Systems for Drinking water. *J. of Envir. Eng. ASCE.*, 112, 744.
- Cooney D. O. and F. P. Strusi (1972). Analytical Describing of Fixed Bed Sorption of Two Langmuir Solutes Under Nonequilibrium Conditions. *Ind. Eng. Chem. Fund.*, 11,123.
- Crittenden J. C. (1976). Mathematical Modeling of Fixed bed Adsorber Dynamic - Single Component and Multicomponent. PH.D. Thesis, Univ. of Michigan, Ann Arbor, MI.
- Crittenden J. C. and W. J. Weber, Jr. (1978). Mathematical Modeling of Fixed Bed Adsorption Systems: Single Component And Multicomponent. 71st Ann. Meeting, Amer. Inst. Chem. Eng., Miami Beach, Florida.
- Crittenden J. C., D. W. Hand, Arora and B. Lykins (1987). *J. Amer. Water Works Assoc.*, 79, 74.
- Crittenden J. C., J. K. Berigan, D. W. Hand and B. Lykins (1987). Design of Rapid Fixed-Bed Adsorption Tests for Nonconstant Diffusivities. *J. of Envir. Eng. ASCE.*, 113, 243.
- Crittenden J. C., T. F. Speth, D. W. Hand, P.J. Luft, B. Lykins (1987). Evaluating multicomponent Competitive Adsorption in Fixed Beds. *J. of Envir. Eng. ASCE.*, 113, 1363.
- Digiano F. A. and W. J. Weber, Jr. (1973). Sorption Kinetics in Infinite Batch Experiments. *J. Water Poll. Control Fed.*, 45, 713.
- Dwiwedi P. N. and Upadyay S. N. (1977). *Ind. Eng. Chem., Process Des. Dev.*, Vol. 16, No. 2, 1977.
- Farmularo J., J. A. Mueller and A. S. Pannus (1980). Predictions of Carbon Column Performance From Pure-Solute Data. *J. Water Poll. Control Fed.* 52, 2019.
- Fettig J. and H. Sontheimer (1987). Kinetics of Adsorption On Activated Carbon: I. Single Solute Systems. *J. of Envir. Eng. ASCE.*, 113, 764.
- Fettig J. and H. Sontheimer (1987). Kinetics of Adsorption On Activated Carbon: II. Multisolute Systems. *J. of Envir. Eng. ASCE.*, 113, 780.
- Fettig J. and H. Sontheimer (1987). Kinetics of Adsorption On Activated Carbon: III. Natural Organic Material. *J. of Envir. Eng. ASCE.*, 113, 795.

- Fritz W., W. Merk, E. U. Schlunder and H. Sontheimer (1980). Competitive Adsorptions of Dissolved Organics on Activated Carbon. In: Activated Carbon Adsorption of Organics From The Aqueous Phase.; Vol. 1. (M. J. McGuire and I. P. Suffet, Eds.). Ann Arbor Sci., Ann Arbor, MI.
- Hall K. R., L. C. Eaglenton, A. Acrivos and T. Vermeulen (1966). Pore and Solid Diffusion in Fixed Beds Adsorption Under Constant Pattern Conditions. Ind. Eng. Chem. Fund. 5, 212.
- Hand D. W., J. C. Crittenden, H. Arora, J. M. Miller and B. Lykins (1987). Designing Fixed-Bed Adsorbents To Remove Mixtures of Organics. J. Amer. Water Works Assoc., 81, 67.
- Heister N. K. and T. Vermeulen (1952). saturation performance of Ion-Exchange and Adsorption Columns. Chem. Eng. Prog., 48, 505.
- Hsieh J. S. C., R. M. turian and C. Tien (1977). Multicomponent Liquid phase Adsorption in Fixed Beds. Amer. Inst. Chem. Eng. J., 23, 263.
- Jain J. S., V. L. Snoeyink (1973). Adsorption From Bislute Systems on Activated Carbon. J. Water Poll. Control Fed.
- Jossens L., J. M. Prausnitz, W. Fritz, E. U. Schlunder and A. L. Myers (1978). Thermodynamics of multisolute Adsorption From Dilute Aqueous Solutions., Chem. Eng. Sci., 33, 1097.
- Keinath T. M. and W. J. Weber, Jr. (1968). A predictive Model for The Design of Fluid Bed Adsorbers. J. Water Poll. Control Fed. 40, 741.
- Keinath T. M. (1977). Design and Operation of Activated Carbon Adsorbers used for Industrial Wastewater Decontamination. Amer. Inst. Chem. Eng. Symp. Ser. 73, 1.
- Kyte W. S. (1973). Nonlinear Adsorption in Fixed Beds. Chem. Eng. Sci. 28, 153.
- Kong E. J. and F. A. Digiano (1986). Competitive Adsorption Among VOCs On Activated Carbon And Carbonaceous Resin. J. Amer. Water Works Assoc., 181.
- Langmuir J. (1918). The Adsorption of Gases on Planes of Glass, Mica, and Platinum. J. Amer. Chem. Soc. 40, 1361.
- Larson A.C. and C. Tien (1983). Multicomponent Liquid Phase Adsorption in Batch. Part 2 Experiment on Carbon Adsorption From Solutions of Phenol, O-cresol, and 2,4-dichlorophenol. Chem. Eng. Commun. 27, 359-361.

- Lee M. C., J. C. Crittenden, V. L. Snoeyink and W. E. Thacker (1980). Mathematical Modeling of Humic Substances Removal With Activated Carbon Beds. National Conference on Environmental Engineering. ASCE., NY.
- Liapis A. I. and D. W. T. Rippen (1978). The simulation of Binary Adsorption in Activated Carbon Columns Using Estimates of Diffusional Resistances within the Carbon Particles Derived From Batch Studies. Chem. Eng. Sci. 35, 593.
- ✱ Mathews A. P. (1975). Mathematical modeling of Multicomponent Adsorption in Batch Reactor. PH.D. Thesis, Univ. of Michigan, Ann Arbor, MI.
- Mathews A. P. and W. J. Weber, Jr. (1977). Effects of External Mass Transfer and Intraparticle Diffusion on Adsorption rates in Slurry Reactors. Amer. Inst. Chem. Eng. Symp. Ser., 73, 91.
- ✱ Mathews A. P. and S. R. Kulkarni (1983). Modification of A Mathematical Model to Take Into Account Particle Size Distribution In Fixed Bed Carbon Adsorption System. Master's Thesis, Kansas State University, Manhattan, KS.
- Mathews A. P. (1983). Adsorption In An Agitated Slurry of Polydisperse Particles. AIChE Symposium Series 79, 18.
- Mathews A. P. and W. J. Weber Jr (1984). Modeling and Parameter Evaluation of adsorption in Slurry Reactors. Chem. Eng. Commun. 25, 157.
- Mathews A. P. and I. Zayas (1989). Particle Size and Shape Effects On Adsorption Rate Parameters. J. of Envir. Eng. ASCE., 115, 41.
- Radke C. J. and J. M. Prausnitz (1972). Adsorption of Organic Solute From Dilute Aqueous Solutions on Activated Carbon. Ind. Eng. Chem. Fund., 11, 445.
- Radke C. J. and J. M. Prausnitz (1972). Thermodynamics of Multisolute Adsorption From Dilute Liquid Solutions. Amer. Inst. Chem. Eng. J., 18, 761.
- Snoeyink, V. L. and W. J. Weber, Jr. (1968). Reaction of The Hydrated Proton With Active Carbon. In: Adsorption From Aqueous Solution, Advances in Chemistry Series, No. 79, 112.
- Smith E. H., S. K. Tseng and W. J. Weber Jr. (1987). Modeling The Adsorption of Target Compounds By GAC In The Presence of Background Dissolved Organic Matter. J. of Envir. Eng. ASCE., 6, 18.
- Speitel G. E. Jr., K. Dovantzis and F. A. Digiano (1987). Mathematical Modeling of Bioregeneration in GAC Columns. J. of Envir. Eng. ASCE., 113, 32.

Speitel, Lu, Turakhia and Zhu. (1989). Biodegradation of Trace Concentrations of Substituted Phenols In GAC Columns. *Envir. Sci. and Tech.*, 23, 68.

Suzuki M. and Kawazoe (1974). Batch Measurement of Adsorption Rate In An Agitated Tank - Pore Diffusion Kinetics With Irreversible Isotherm. *J. Chem. Eng. Japan*, 7, 346.

Sweeny M. W., W. A. Melville, B. Trogovicinh and C. P. L. Grady, Jr. (1982). Adsorption Isotherm Parameter Estimation.

Thacker W. E. and V. L. Snoeyink (1978). On Evaluating Granular Activated Carbon Adsorption. Notes and Comments, *J. Amer. Water Works Assoc.*, 70, 45.

Traegner U. K. and M. T. Suidan (1989). Parameter Evaluation for Carbon Adsorption. *J. Envir. Eng. ASCE.*, 115, 109.

Van Hall C. E., Ed. Measurements of Organic Pollutants in Water and Wastewater Treatment. ASTM Spec. Pub. 686 (Philadelphia: American Society for Testing and Materials, 1979).

Van Vliet, B. M. and W. J. Weber, Jr (1979). Comparative Performance of Synthetic Adsorbents and Activated Carbon for Specific Compound Removal From wastewaters. 52nd Ann. Conf., Water Poll. Control Fed., Houston, TX.

Van Vliet B. M. and W. J. Weber, Jr (1980). Modeling and Prediction of Specific Compound Adsorption by Activated Carbon. *Water Research*, 14, 1719.

Vermeulen T. (1953). Theory for Irreversible and Constant Pattern Solid Diffusion. *Ind. Eng. Chem. Fund.*, 45.

Voudrias E. A., V. L. Snoeyink and R. A. Larson (1986). Desorption of Organic Formed On Activated Carbon., *J. Amer. Water Works Assoc.*, 78, 82.

Weber W. J. Jr. Physicochemical Process For Water Quality Control. (1972), Wiley-Interscience.

Weber W. J. Jr. and R. R. Rumner (1965). Intraparticle Transport of Sulphonated Alkyl Benzenes in a Porous Solid: Diffusion with NonLinear Adsorption. *Water Resources Res.*, 1, 361.

Watermark M. (1975). Kinetics of Activated Carbon Adsorption. *J. Water Poll. Control Fed.*, 47, 704.

Wilmanski K. and K. Lipinski (1989). Adsorption Kinetics In GAC Systems for Wastewater Treatment. *J. of Envir. Eng. ASCE.*, 115, 91.



Zwiebel I., R. L. Gariepy and J. J. Schnitzer (1972). Fixed Bed Desorption Behavior of Gases with Non-Linear Equilibria: Part 1. Dilute, One Component Isotherm Systems. Amer. Inst. Chem. Eng. J., 18,1139.